Available online at www.eccomasproceedia.org
Eccomas Proceedia COMPDYN (2017) 459-469

ECCOMAS
Proceedia

COMPDYN 2017
6th ECCOMAS Thematic Conference on
Computational Methods in Structural Dynamics and Earthquake Engineering
M. Papadrakakis, M. Fragiadakis (eds.)
Rhodes Island, Greece, 15–17 June 2017

ENERGY HARVESTING IN A NONLINEAR SYSTEM UNDER HARMONIC AND RANDOM EXCITATIONS

Tiago L. Pereira[1], Aline S. De Paula[1], Adriano T. Fabro[1], Marcelo A. Savi[2]

[1] Universidade de Brasília, Department of Mechanical Engineering
70.910.900 – Brasília – DF, Brazil
e-mail: tiagolei.tl@gmail.com, alinedepaula@unb.br, fabro@unb.br

[2] Universidade Federal do Rio de Janeiro, COPPE , Department of Mechanical Engineering
21.941.972 – Rio de Janeiro – RJ, Brazil, P.O. Box 68.503
savi@ufrj.br

Keywords: Piezoelectric, nonlinear system, energy harvesting, random excitation

Abstract. *Smart material has the ability to convert energy between two distinct physical domains. Piezoelectric material are an example of this material, the vibration-based energy harvesting using piezoelectric elements is possible by exploring the direct effect, where the piezoelectric material is able to convert mechanical in to electrical energy. This application can be very useful for applications in powering small electronic devices. The energy harvesting system presented in this work is a magnetoelastic structure that consists of a ferromagnetic cantilevered beam with two permanent magnets, one located in the free end of the beam and the other at a vertical distance d from the beam free end. In order to use this device as a piezelectric power generator, two piezoceramic layers are attached to the root of the cantilever and a bimorph generator is obtained. The piezomagnetoelastic structure is subjected to a combination of harmonic and random excitations. The parameter Noise-to-Signal Ratio (NSR) is used in order to quantify different combinations of the forcing terms. A method to evaluate the harvested energy and the performance of the piezomagnetoelastic structure is proposed. The method is applicable both to deterministic and to non-deterministic signals and is based on the Power Spectral Density (PSD) of the input, dimensionless force, and the output signal, dimensionless electrical voltage. Numerical simulations are carried out identifying better combinations of harmonic and random excitations for energy harvesting purposes.*

Peer-review under responsibility of the organizing committee of COMPDYN 2017.
doi: 10.7712/120117.5432.17603

1 INTRODUCTION

Smart material are capable to convert energy between two distinct physical domains. The piezoelectric material are smart material that, due to the atomic configuration, convert mechanical energy into electric energy and vice-versa. The direct effect of a piezoelectric material is when a mechanical energy is converted into electrical energy, while the inverse effect is when electrical energy is converted into mechanical energy. Typically, the piezoelectric material can act as a sensor and actuator exploring, respectively, direct and inverse effects. Another application associated with the direct effect is energy harvesting from mechanical vibration.

Some devices were developed with the aim of harvesting environment vibration energy using piezoelectric materials. Some researches focused on harvesting the energy available in human walk movement. In this context, [1,2] investigated a system that can be used in backpack, and Shenck [3] proposed a device to use in shoes. Sohn [4] proposed a device to harvest energy from the blood pressure variation. The electrical coupling of the piezoelectric system is a point that has been investigated [5].

Several proposed devices are linear and considers harmonic excitation. In this case, it is required an excitation in a resonance frequency, as can be seen in the work of Roundy and Zhang [6]. When the system is excited in a frequency slightly different from the resonance frequency, however, the electrical response is drastically reduced. Thereby some work focus on obtaining a broadband energy harvester by using nonlinearities. Mann [7] suggested a bistable system with magnetic interaction, a system with a nonlinear damping was proposed by Tehrani [8], while Litak [9] proposed an inverted beam with a tip mass.

Some researches focus on the influence of a random excitation in energy harvesting using nonlinear systems. Litak [10] verified that a bistable structure has a stochastic resonance when excited with a white noise excitation. De Paula [11] experimentally investigated the system when subjected to a random excitation and showed some remarkable points, comparing the linear, nonlinear monostable and nonlinear bistable configuration. The energy harvested is bigger in the nonlinear bistable configuration and when oscillate around the both stable equilibrium points. In addition, Ferrari [12] presented a study with the nonlinear system under random excitation that show that for bistable system the RMS voltage is bigger than the monostable configuration.

In real problems, it is usual to have presence of noise in a harmonic excitation. This work presents an analyzes of a bistable piezomagnetoelastic structure under combined harmonic and random excitations. Energy harvesting and system performance are evaluated by a proposed method based on Power Spectral Density (PSD), that uses information of input (mechanical excitation) and output (voltage).

2 PIEZOMAGNETOELASTIC STRUCTURE

The studied energy harvesting system is based on a magnetoelastic structure, first investigated by Moon and Holmes [13]. Figure 1 presents a schematic representation of the structure that consists of a ferromagnetic cantilevered beam with two permanent magnets, one located in the free end of the beam and the other at a vertical distance d from free end, due to the magnets the system present a nonlinear configuration. Erturk [14] adapted the system in order to use the device as a piezoelectric power generator by attaching two piezoceramic layers to the root of the cantilever beam. Thus, a bimorph generator is obtained and the system can harvest the energy of an environment under vibration conditions. This work considers a base excitation, with combined harmonic and random motions.

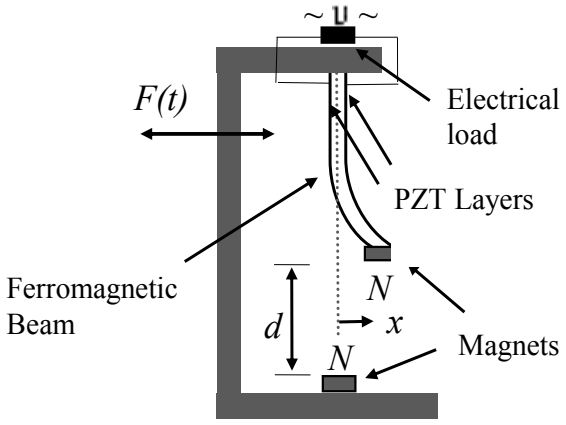

Figure 1: Schematic representation of the piezomagnetoelastic structure.

The system has two degree of freedom, one mechanical and one electrical. Thus, the equations of motion present electro-mechanical coupling. The system is governed by Eqs. (1) and (2).

$$\ddot{x} + 2\zeta\dot{x} - \frac{1}{2}\,x(1 - x^2\,) - \chi v = F(t), \tag{1}$$

$$\dot{v} + \lambda v + \kappa\dot{x} = 0, \tag{2}$$

where x is the dimensionless tip displacement of the beam in the transverse direction, v is the dimensionless voltage across the load resistance. The constant ζ is the mechanical damping ratio, χ is the dimensionless piezoelectric coupling term in the mechanical equation, κ is the dimensionless piezoelectric coupling term in the electrical circuit equation, and λ is the reciprocal of the dimensionless time constant ($\lambda \propto 1/R_L C_P$ where R_L is the load resistance and C_P is the equivalent capacitance of the piezoceramic layers).

The values of the parameters are considered as the same as in Erturk [14] :$\zeta = 0.01$, $\chi = 0.05$, $\kappa = 0.5$ and $\lambda = 0.05$. By considering these parameters, the equilibrium points, obtained from Eqs. (1) and (2), are two stable spiral points located at $(x, \dot{x}, v) = (\pm 1,0,0)$ and one unstable saddle point located at $(x, \dot{x}, v) = (0,0,0)$. $F(t)$ is the system excitation and consists in a combination of harmonic and random signals. For the harmonic excitation contribution it is considered $F(t) = f_0 \cos(\omega t)$, where f_0 is the dimensionless excitation due to base acceleration ($f_0 \propto \Omega^2 X_0$ where X_0 is the dimensionless base displacement amplitude), and for the random excitation contribution it is considered $F(t\,) = N(\sigma, \bar{x})$, that is a Gaussian white noise with mean value $\bar{x}$ and standard-deviation σ. The total excitation is shown in Eq. (3).

$$F(t) = f_0 \cos(\omega t) + N(\sigma, \bar{x}) \tag{3}$$

In order to measure different combinations of the random and harmonic excitations it is established the parameter Noise to Signal Ratio (NSR), shown in Eq. (4).

$$NSR = \frac{\sigma}{f_0} \tag{4}$$

3 METHOD TO EVALUATE HAVESTED ENERGY AND SYSTEM PERFORMANCE

To evaluate the harvested energy and system performance we propose the analysis based on the Power Spectral Density (PSD). The PDS, defined in Eq. (6), is the distribution of power in frequency domain.

$$\hat{x}(\omega) = \int_{-\infty}^{\infty} e^{-2\pi i\omega t} x(t) dt \tag{5}$$

$$PSD = |\hat{x}(\omega)|^2 \tag{6}$$

where $\hat{x}(\omega)$ is the Fourier Transform. The PSD is calculated using a periodogram approach and Hanning windowing [15]. The area under the curve of PSD is defined in this work as Power of the Signal (PS). PS of excitation (PS_f) and voltage (PS_v) are estimated and it is established the ratio, r, of PS_v and PS_f as a parameter to measure the performance of the system.

$$r = \frac{\int_0^{\omega} PSD_v(\omega) d\omega}{\int_0^{\omega} PSD_f(\omega) d\omega} = \frac{PS_v}{PS_f}, \tag{7}$$

The bigger the value of the ratio r, the larger the area under the PSD of electrical response when compared to the mechanical input. Moreover, the value of PSD_v is related to electrical output. Thus, PS_v and r are parameters used to indicate system performance for different dynamical behavior. The quantities $v(t)$ and $F(t)$ are dimensionless, so the PS_v and PS_f can be compared directly. The parameter PS_v is used to quantify the energy harvesting and the parameter r is used to evaluate system performance. It is important to highlight that the proposed method is appropriate for both deterministic and non-deterministic signals.

4 DYNAMICAL ANALYSIS

The dynamical analysis presented in this section verify different combinations of harmonic and random excitations and considers different values of forcing amplitude and frequency. The analysis begins for predominant harmonic excitation, thus, small NSR. The value of NSR is increased until it is considered the random excitation becomes predominant.

4.1 Varying the forcing amplitude

To construct the bifurcation diagrams presented in Figure 2 two coexisting behaviors are considered at $f_0 = 0.083$ and $\omega = 0.8$, identified when there is no noise (NSR=0). Pink points are related to a period-1 response obtained with initial conditions $[x(0), \dot{x}(0), v(0)] = [1,1,0]$, while black points are related to a chaotic behavior obtained with initial condition $[x(0), \dot{x}(0), v(0)] = [1,0,0]$. Note that this forcing amplitude is in the middle of the bifurcation diagram. From these two reference behaviors, forcing amplitude is increased and decreased and plotted together in the diagram. Thus, 4 procedures are together in the same figure. From Figure 2 (a) to Figure 2 (f) NSR is continuously increased so that the influence of the random excitation, in an initially pure harmonically excited system, can be analyzed.

Figure 2 (a) presents a pure harmonically excited system (NSR=0). It can be observed that the period-1 orbit keep stable for a large range of forcing amplitude. From black point, one can observe two regions that indicates a chaotic response and a periodic window, with a period-5 orbit. For f_0 bigger than approximately 0.11 only one period-1 orbit is stable (the same identified from the pink points), while for values smaller than around 0.78 two period-1 orbit coexists.

When NRS is increased to 0.05, the region related to the period-5 orbit is replaced by a chaotic behavior, as shown in Figure 2 (b). This is the main difference in the global behavior of the system when compared to the situation when NSR=0.

Figure 2 (c) shows the response to NSR=0.3. Note that pink points now fill a bigger region in the bifurcation region, this happens because the Poincaré section has a dispersion of the points but the qualitatively response in phase space is the same. From black point, we observe the chaotic behavior region is enlarged.

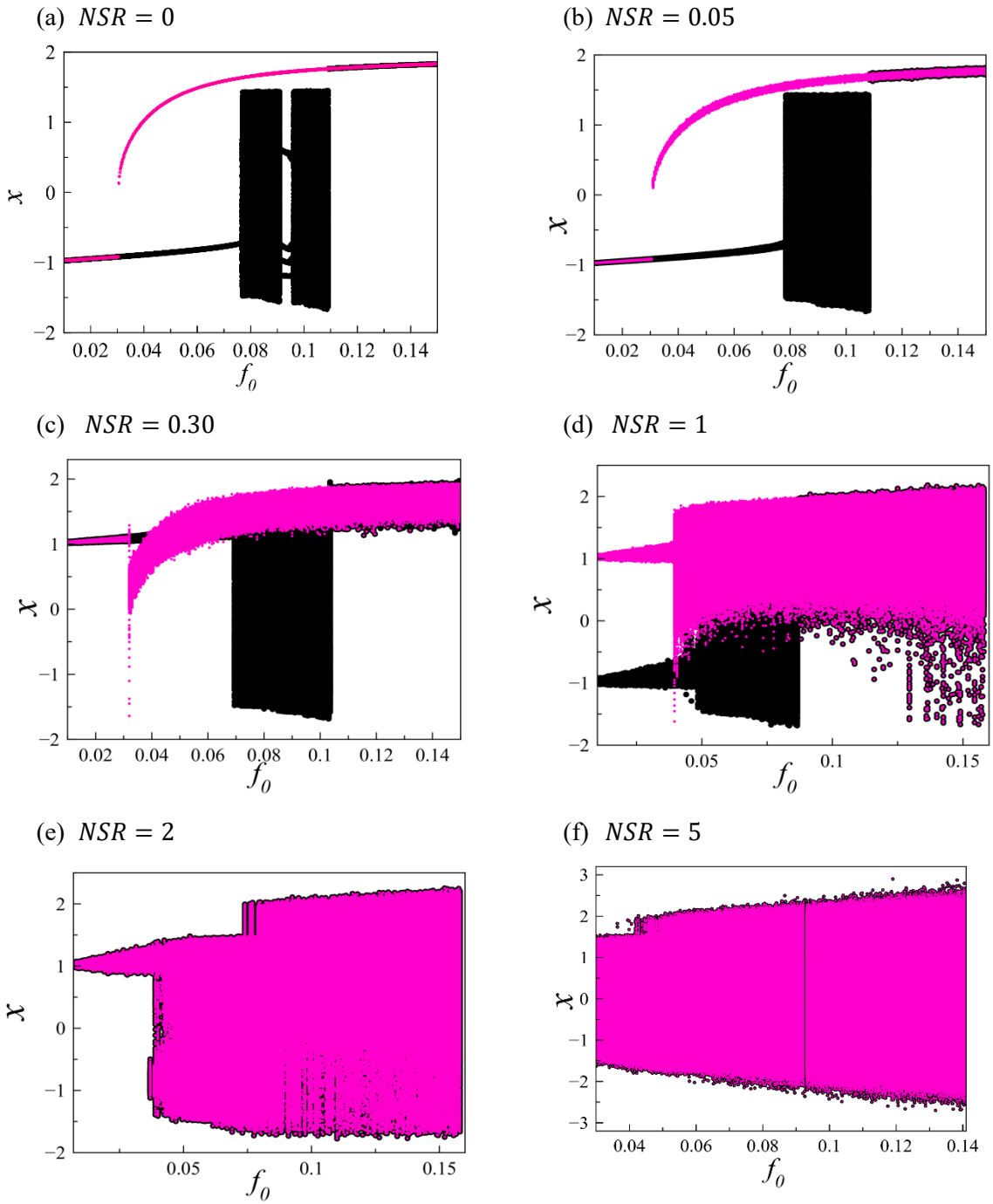

Figure 2 Bifurcation Diagram for different levels of combination of forcing and varying the amplitude.

With NSR=1, system response changes considerably. For values of $f_0 < 0.04$, bifurcation diagram identifies two coexistent behaviors that are symmetric, in both of them the tip of the beam oscillates around only one stable equilibrium point. For higher values of f_0 system oscillates around both stable equilibrium point and there is coexistence of behaviors.

The coexistence of behavior disappears when $NSR = 2$, as seen in the Figure 2 (e). At this point just two behaviors are observed, for smaller values of forcing amplitude system oscillates around only one stable equilibrium point, while for higher amplitudes the response fill all phase space. Due to the presence of noise, Poincaré section does not present lamellar structure for any forcing amplitude. For 5, the same kind of behavior is observed in all range of analyzed forcing amplitude, as shown in Figure 2 (f). Thus, we assume random excitation is predominant.

4.2 Varying the forcing frequency

In this section a similar analysis presented for forcing amplitude variation is carried on, now considering variation of forcing frequency, ω. In the bifurcation diagrams presented in Figure 3 pink points are related to a period-1 response obtained with initial conditions $[x(0), \dot{x}(0), v(0)] = [1,1,0]$, while black points are related to a chaotic behavior obtained with initial condition $[x(0), \dot{x}(0), v(0)] = [1,0,0]$ at $f_0 = 0.083$ and $\omega = 0.8$. From these two coexisting attractors, the forcing frequency is increased and decreased. This 4 procedures are plotted together in each diagram.

For $NSR = 0$, the same reference bifurcation diagram shown in Figure 2(a) is presented in Figure 3 (a).

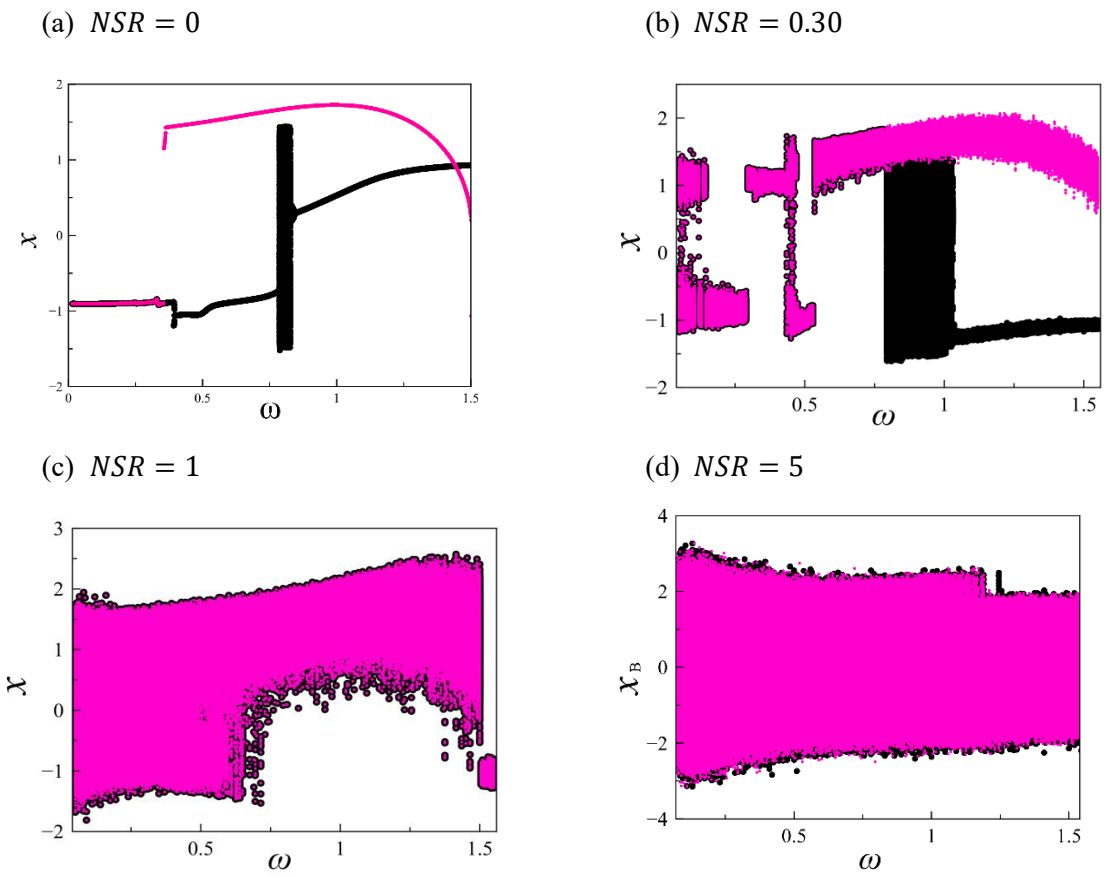

Figure 3. Bifurcation Diagram for different levels of combination of forcing and varying the frequency.

Increasing NSR to 0.3, as presented in Figure 3 (b), considerable changes occur. For $\omega < 0.5$, behaviors related to pink and black points consist of oscillations around just one equilibrium point. Note that there are two coexisting attractors, one has Poincaré section points around x=-1 and the other around x=1. For $\omega > 0.5$, we observe similar behavior to the one presented in Figura 2(c), pink points represents a dispersion of the points in a response that oscillates around both stable equilibrium points, while black points are related to chaotic behavior. Even with the presence of noise, the Poincaré section presents a lamellar structure.

For $NSR = 1$, shown in Figure 3 (c), the coexistence of behavior disappears, and two distinct behaviors are presented. For smaller values of forcing excitation all Poincaré section is filled with no pattern, as well as the phase space. For higher values of f_0 system oscillates around both stable equilibrium point always with big oscillation amplitudes. This behavior will be explored in the next section. In Figure 3 (d), for NSR=5, we assume random excitation is predominant as in the case presented in Figure 2(f).

5 ENERGY HARVESTING AND PERFORMANCE ANALYSIS

This section aims to analyze the harvested energy and the performance of the piezomagnetoelastic system. From all responses presented in the section 4, five reference responses (identified when NSR = 0) are chosen: period-1 orbit oscillating around both stable equilibrium points, another period-1 orbit oscillating around both stable equilibrium points, period-1 orbit oscillating around only one stable equilibrium point, and chaotic. The dynamic evolution of these reference orbits are analyzed when NSR is increased.

The analysis of the first case, period-1 orbit oscillating around two stable equilibrium point, is exhibited in the Figure 4. This response is obtained with $f_0 = 1.4$ and $\omega = 0.1$. Figure 4(a) and (b) presents values of PS and r, respectively, when NSR is increased from 0 to 3. Figure 4 (a) also illustrates the kind of behavior presented by the system in phase space (blue) together with Poincaré section (pink). Note that the reference response occurs until NSR=1 and, after a transition region (hatched), a different type of behavior is obtained, where phase space is all filled. It is important to highlight that the presented phase spaces and Poincaré sections are obtained for fixed values of NSR, however, each one is used to represent the qualitative behavior presented by the system in a range of NSR. Note that the first region (0 < NSR < 1) is more appropriated to harvest energy due to higher value of PS_v. Moreover, by considering value of r, the performance of the system is better for smaller values of NSR.

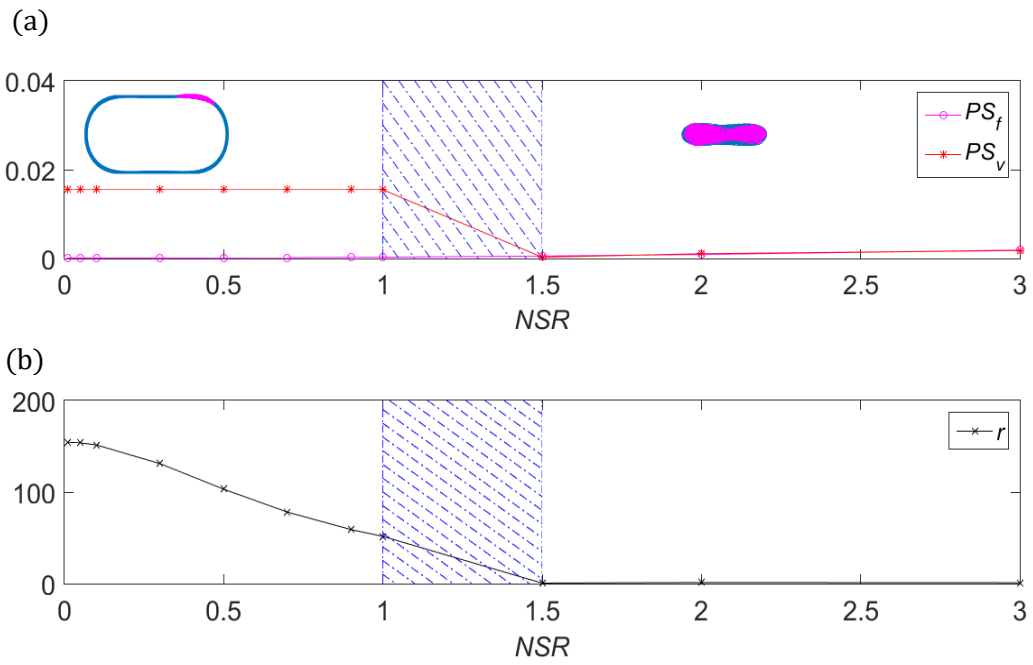

Figure 4. System behavior when NSR is increased from 0 to 3 by considering the first reference orbit. (a) *PSf, PSv* and qualitative response of the system; (b) *r*.

The same analysis presented in Figure 4 is now carried out for the second reference situation, another period-1 orbit oscillating around just one stable equilibrium point, as presented in Figure 5. Harmonic forcing parameters are $f_0 = 0.1$ and $\omega = 0.8$. By comparing Figures 4 and 5, note that the first reference orbit has better performance and is more suitable for energy harvesting than this second orbit. This can be explained by higher oscillations amplitudes of the first reference orbit. From Figure 5, observe that the first region is better for energy harvesting, PS_v, and presents the best performance, r. In the interval of $NSR = 0.3$ to $NSR = 0.5$ emerge a behavior that oscillate around just one equilibrium point, that is not convenient for energy harvesting purpose. For $NSR > 0.7$ the system oscillates without any pattern, filling all phase space.

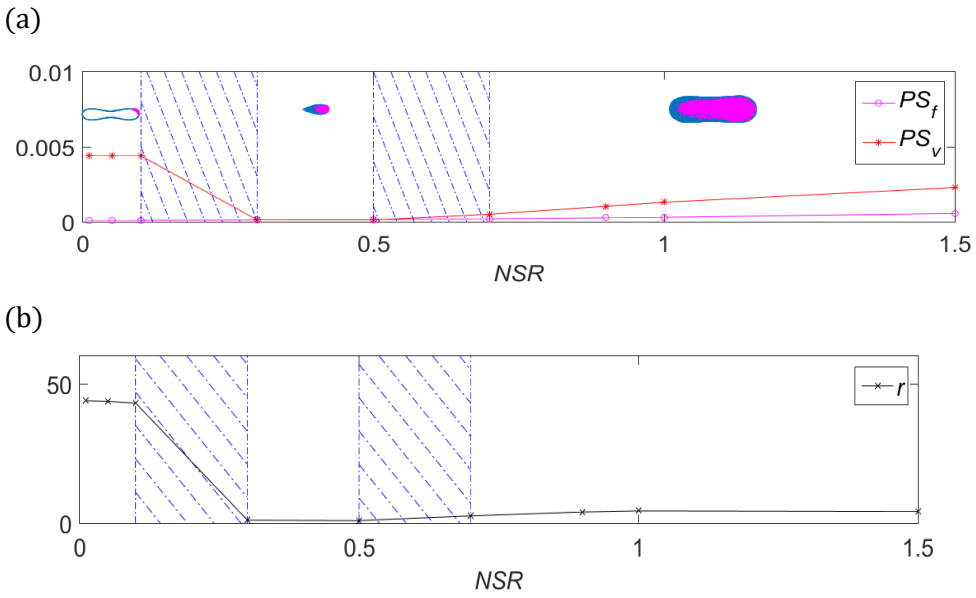

Figure 5. System behavior when NSR is increased from 0 to 300% by considering the second reference orbit. (a) *PSf, PSv* and qualitative response of the system; (b) *r*.

Figure 6 presents the analysis for the third reference orbit. Harmonic forcing parameters are $f_0 = 0.063$ and $\omega = 0.8$. Note that the initial behavior is not appropriate to harvest energy, presenting the lowest PS_v and r of reference orbits. When $NSR = 0.5$ system response changes, increasing the harvested energy and system performance. For this case the performance r achieves the best value when $NSR = 1$.

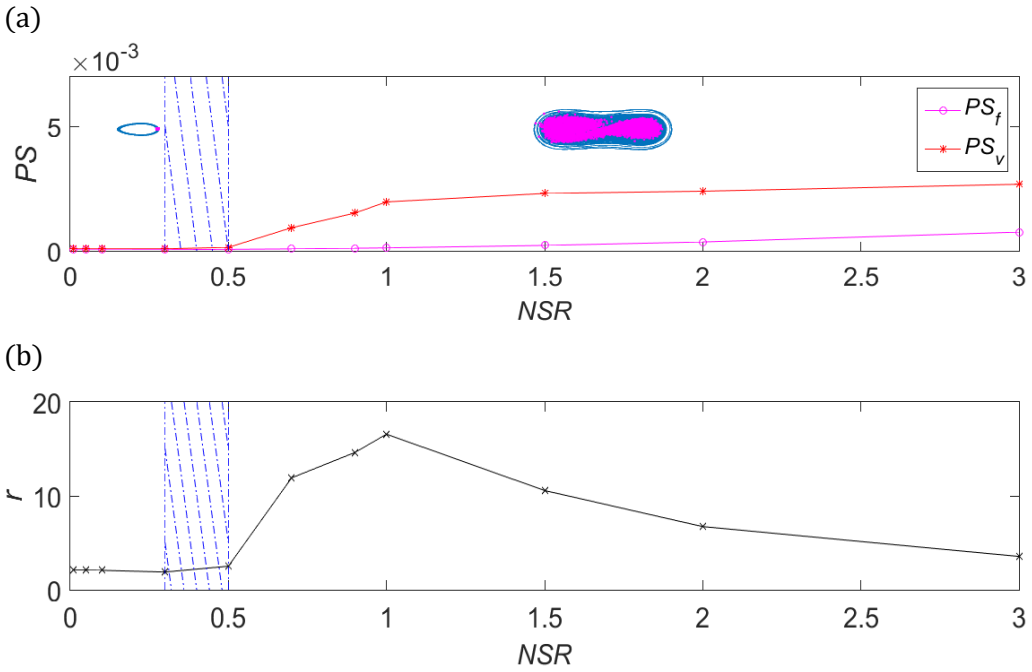

Figure 6. System behavior when NSR is increased from 0 to 3 by considering the third reference orbit. (a) PS_f, PS_v and qualitative response of the system; (b) *r*.

Figure 7 presents the evolution for the last reference case, a chaotic response. Harmonic excitation parameters are $f_0 = 0.083$ and $\omega = 0.8$. By increasing NSR, after a transition region (hatched), system presents a response that oscillates around both stable equilibrium points with large amplitudes. This behavior presents the best performance and harvested energy as can be observed by values of PS_v and r. For values of $NSR > 2$, a different behavior is observed. By comparing this response with the chaotic one, the value of PS_v is bigger but with a smaller r, once more mechanical energy is provided to the system as the noise increases.

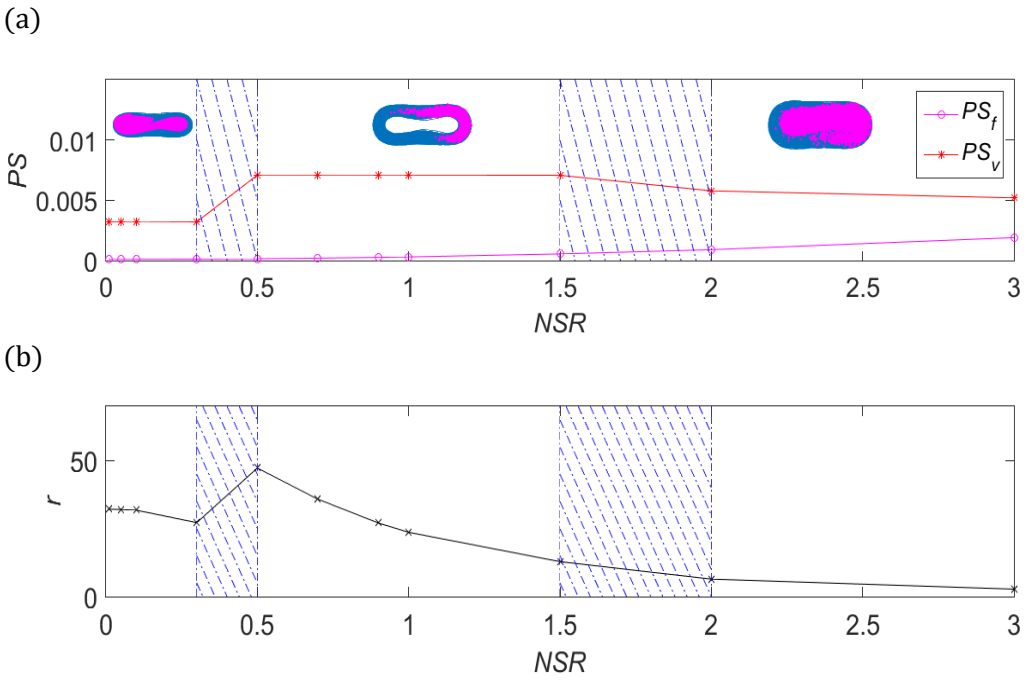

Figure 7. System behavior when NSR is increased from 0 to 3 by considering the fourth reference orbit. (a) PS_f, PS_v and qualitative response of the system; (b) r.

6 CONCLUSIONS

In this work a nonlinear model for a piezomagnetoelastic structure is presented. System response is evaluated for a combination of harmonic and random excitations considering a bistable configuration. A richness dynamical response is observed.

After evaluating the global dynamical behavior for different harmonic forcing parameters and different values of NSR, four reference orbit (chosen when NSR=0) are chosen. Beginning from these orbits, the harvested energy and system performance are evaluated when NSR is increased. The increase of NSR promotes qualitative changes in system response and more suitable responses for energy harvesting proposes are identified. The better behavior occurs when the tip of the beam oscillates around both stable equilibrium points with the largest oscillation amplitude for the biggest period of time. Moreover, proper combination of harmonic forcing parameters and NSR lead to the this desired behavior.

REFERENCES

The authors would like to thank the Brazilian Research Agencies CNPq, CAPES and Fundação de Apio a Pesquisa do Distrito Federal FAPDF for the support.

REFERENCES

[1] Rome LC, Flynn L, Goldman EM, Yoo TD. Generating electricity while walking with loads. Science 2005;309:1725–8. doi:10.1126/science.1111063.

[2] Feenstra J, Granstrom J, Sodano H. Energy harvesting through a backpack employing a mechanically amplified piezoelectric stack. Mech Syst Signal Process 2008;22:721–34. doi:10.1016/j.ymssp.2007.09.015.

[3] Shenck NS, Paradiso JA. Energy scavenging with shoe-mounted piezoelectrics. IEEE Micro 2001;21:30–42. doi:10.1109/40.928763.

[4] Sohn JW, Choi SB, Lee DY. An investigation on piezoelectric energy harvesting for MEMS power sources. ResearchGate 2005;219:429–36. doi:10.1243/095440605X16947.

[5] S. Tol FLD. Piezoelectric power extraction from bending waves: Electroelastic modeling, experimental validation, and performance enhancement. Wave Motion 2015;60. doi:10.1016/j.wavemoti.2015.08.008.

[6] Roundy S, Zhang Y. Toward self-tuning adaptive vibration-based microgenerators. vol. 5649, 2005, p. 373–84. doi:10.1117/12.581887.

[7] Mann BP, Owens BA. Investigations of a nonlinear energy harvester with a bistable potential well. J Sound Vib 2010;329:1215–26. doi:10.1016/j.jsv.2009.11.034.

[8] Ghandchi Tehrani M, Elliott SJ. Extending the dynamic range of an energy harvester using nonlinear damping. J Sound Vib 2014;333:623–9. doi:10.1016/j.jsv.2013.09.035.

[9] Grzegorz Litak MIF. Regular and chaotic vibration in a piezoelectric energy harvester. Meccanica 2015. doi:10.1007/s11012-015-0287-9.

[10] Litak G, Friswell MI, Adhikari S. Magnetopiezoelastic energy harvesting driven by random excitations. Appl Phys Lett 2010;96:214103. doi:10.1063/1.3436553.

[11] De Paula AS, Inman DJ, Savi MA. Energy harvesting in a nonlinear piezomagnetoelastic beam subjected to random excitation. Mech Syst Signal Process 2015;54–55:405–16. doi:10.1016/j.ymssp.2014.08.020.

[12] Ferrari M, Baù M, Guizzetti M, Ferrari V. A single-magnet nonlinear piezoelectric converter for enhanced energy harvesting from random vibrations. Sens Actuators Phys 2011;172:287–92. doi:10.1016/j.sna.2011.05.019.

[13] Moon FC, Holmes PJ. A magnetoelastic strange attractor. J Sound Vib 1979;65:275–96. doi:10.1016/0022-460X(79)90520-0.

[14] Erturk A, Hoffmann J, Inman DJ. A piezomagnetoelastic structure for broadband vibration energy harvesting. Appl Phys Lett 2009;94:254102. doi:10.1063/1.3159815.

[15] Newland DE. An Introduction to Random Vibrations and Spectral Analysis. 2nd edition. London ; New York: Longman; 1984.